ELSEVIER

Surface Science 377–379 (1997) 294–300

surface science

Electron energy loss for isolated cylinders

J.M. Pitarke [a,*], A. Rivacoba [b]

[a] *Materia Kondentsatuaren Fisika Saila, Zientzi Falkultatea, Euskal Herriko Unibertsitatea, 644 Posta kutxatila, 48080 Bilbo, Basque Country, Spain*

[b] *Materialen Fisika Saila, Kimika Falkultatea, Euskal Herriko Unibertsitatea, 1072 Posta kutxatila, 20080 Donostia, Basque Country, Spain*

Received 1 August 1996; accepted for publication 9 September 1996

Abstract

The interaction of STEM electrons with cylindrical surfaces is investigated within the framework of the self-energy formalism. The energy loss is studied as a function of the impact parameter and for the case of broad beam geometries. An expression for the effective inverse longitudinal dielectric function of isolated cylinders is derived, and applications of this theory are reviewed.

Keywords: Electron–solid interactions, scattering, diffraction; Many body and quasi-particle theories

1. Introduction

Since the original paper by Ritchie [1], surface plasmons have been the subject of continuing interest. In particular, electron energy-loss spectroscopy in scanning transmission electron microscopy (STEM) has become a powerful tool for investigating the properties of these surface collective excitations. In a typical STEM configuration a well-focused probe of electrons is used to yield electron energy-loss spectra, and both the energy position and the strength of the energy-loss peaks provide information on the characteristic bulk and surface plasmons of the solid. Energy-loss spectra have been calculated for electrons moving at fixed impact parameters from given planar interfaces [2], spheres [3], cylinders [4–6] and more complex geometries [7–9].

In the case of electrons incident on inhomogeneous media which pass at random distances from the particles, effective medium theories have been used, and the concept of the effective dielectric response has been introduced. The $q=0$ limit of this average dielectric function for a system of spherical particles was first derived by Maxwell-Garnett [10], within a mean field approximation valid for small values of the volume occupied by the spheres. Fujimoto and Komaki [11] included all multipoles to derive, within the hydrodynamic approximation for a free-electron gas, the energy loss of a broad beam of fast electrons incident on an isolated sphere. This result for the energy loss was later generalized to obtain, in the frame of both classical [12] and quantal [13] theories, an expression that is valid for any local dielectric function inside the sphere. Recently, an expression for the effective longitudinal dielectric function of a random system of identical spherical particles has been derived, within a mean field approximation [14].

* Corresponding author.

PII S0039-6028(96)01400-8

For cylindrical interfaces all previous works focused on probes traveling on a definite trajectory, and only very recently has a broad beam geometry been considered to investigate the experimental valence loss spectra from zeolites [15]. The discovery of tubular fullerenes [16], a few years ago, has opened a new focus of interest for the application of these theories [17].

In this paper we investigate the interaction of STEM electrons with isolated cylindrical interfaces, within the framework of the self-energy formalism [13]. The energy loss is first studied as a function of the impact parameter. Then, the case of a broad beam geometry is considered, and a momentum-dependent effective inverse longitudinal dielectric function is derived by equating the energy-loss probability of electrons passing through the composite with the bulk energy-loss probability. Finally, a spectral representation of the effective inverse dielectric function is given, and surface mode strengths and positions are analyzed.

2. Theory

We consider a swift electron interacting with an inhomogeneous medium. Target excitations together with the reaction of the probe to these excitations can be described by the self-energy of the probe. For an incoming particle in a state $\phi_0(\boldsymbol{r})$ of energy E_0 one writes [18]:

$$\Sigma_0 = \int \mathrm{d}^3\boldsymbol{r} \int \mathrm{d}^3\boldsymbol{r}' \phi_0^*(\boldsymbol{r}) \Sigma(\boldsymbol{r},\boldsymbol{r}',E_0)\phi_0(\boldsymbol{r}'), \tag{1}$$

where $\Sigma(\boldsymbol{r},\boldsymbol{r}',E_0)$ represents the non-local self-energy. In the so-called GW approximation [19,20]:

$$\Sigma(\boldsymbol{r},\boldsymbol{r}',E_0) = \frac{i}{\hbar}\int \frac{\mathrm{d}E'}{2\pi} G(\boldsymbol{r},\boldsymbol{r}',E_0-E')W(\boldsymbol{r},\boldsymbol{r}',E'), \tag{2}$$

$G(\boldsymbol{r},\boldsymbol{r}',E)$ and $W(\boldsymbol{r},\boldsymbol{r}',E)$ being the Green function for the probe and the time-ordered screened interaction, respectively. In applying this formula we replace $G(\boldsymbol{r},\boldsymbol{r}',E)$ by the zero order approximation. For STEM electrons moving with velocities that are large with respect to the velocities of target electrons the effect of the Pauli restriction can be neglected, and one writes:

$$G^0(\boldsymbol{r},\boldsymbol{r}',E) = \hbar \sum_f \frac{\phi_f^*(\boldsymbol{r}')\phi_f(\boldsymbol{r})}{E-E_f+i\delta}, \tag{3}$$

where the sum is extended over a complete set of final states $\phi_f(\boldsymbol{r})$ of energy E_f, and δ is a positive infinitesimal.

The damping rate, γ, experienced by the particle as a consequence of the interaction with real excitations of the target, is directly related to the imaginary part of Σ_0:

$$\gamma = -\frac{2}{\hbar}\,\mathrm{Im}\,\Sigma_0. \tag{4}$$

Thus, introduction of Eq. (1) into Eq. (4) gives, after some rearrangement:

$$\gamma = \int_0^\infty \mathrm{d}\omega\, P_\omega, \tag{5}$$

where P_ω represents the so-called energy-loss probability for the probe to transfer energy $\hbar\omega$ to the medium:

$$P_\omega = -2\sum_f \int \mathrm{d}\boldsymbol{r} \int \mathrm{d}\boldsymbol{r}'\, \phi_f^*(\boldsymbol{r}')\phi_0(\boldsymbol{r}')\phi_f(\boldsymbol{r})\phi_0^*(\boldsymbol{r}) \times \mathrm{Im}\, W^{\mathrm{ind}}(\boldsymbol{r},\boldsymbol{r}',\omega)\delta[\hbar\omega-(E_0-E_f)], \tag{6}$$

$W^{\mathrm{ind}}(\boldsymbol{r},\boldsymbol{r}',\omega)$ being the retarded induced screened interaction.

2.1. Definite trajectories

In the case of electrons moving on a definite trajectory along the z axis at a given impact parameter $\boldsymbol{b}$, the initial and final states can be described by taking a δ function in the transverse direction and plane waves in the direction of motion. Introduction of these states, $\phi_0(\boldsymbol{r})$ and $\phi_f(\boldsymbol{r})$, into Eq. (6) and neglect of the electron recoil gives:

$$P_\omega = -\frac{1}{\pi\hbar vL}\int \mathrm{d}\boldsymbol{r} \int \mathrm{d}\boldsymbol{r}'\, \mathrm{e}^{-i\omega/v(z-z')} \times \delta(\rho-\boldsymbol{b})\delta(\rho'-\boldsymbol{b})\,\mathrm{Im}\, W^{\mathrm{ind}}(\boldsymbol{r},\boldsymbol{r}';\omega), \tag{7}$$

L being the normalization length, v, the velocity of the electron, and ρ and ρ', components of $\boldsymbol{r}$ and $\boldsymbol{r}'$ in a plane perpendicular to the z axis.

Our system consists of an infinite cylinder of radius a and local dielectric function ϵ_ω centered in a box of dielectric function ϵ_0 and volume $\Omega\to\infty$, the axis of the cylinder being parallel to the trajectory of the electron, along the z axis. The induced interaction, $W^{\rm ind}(\boldsymbol{r}=\boldsymbol{b},\boldsymbol{r}'=\boldsymbol{b};\omega)$, is easily obtained by imposing the boundary conditions at $\rho=a$, and Eq. (7) gives [6]:

$$P_\omega=\frac{2e^2}{\pi\hbar v}\,{\rm Im}\left\{(\epsilon_\omega^{-1}-\epsilon_0^{-1})\right.$$

$$\times\sum_{m=0}^{\infty}\mu_m\left[I_m\left(\frac{\omega b}{v}\right)K_m\left(\frac{\omega b}{v}\right)\right.$$

$$\left.\left.+\frac{\epsilon_0 K_m\left(\frac{\omega a}{v}\right)K_m'\left(\frac{\omega a}{v}\right)I_m^2\left(\frac{\omega b}{v}\right)}{\epsilon_\omega I_m'\left(\frac{\omega a}{v}\right)K_m\left(\frac{\omega a}{v}\right)-\epsilon_0 I_m\left(\frac{\omega a}{v}\right)K_m'\left(\frac{\omega a}{v}\right)}\right]\right\},\tag{8}$$

for inside trajectories, and

$$P_\omega=-\frac{2e^2}{\pi\hbar v}\,{\rm Im}\left\{(\epsilon_\omega^{-1}-\epsilon_0^{-1})\sum_{m=0}^{\infty}\mu_m\right.$$

$$\left.\times\frac{\epsilon_\omega I_m\left(\frac{\omega a}{v}\right)I_m'\left(\frac{\omega a}{v}\right)K_m^2\left(\frac{\omega b}{v}\right)}{\epsilon_\omega I_m'\left(\frac{\omega a}{v}\right)K_m\left(\frac{\omega a}{v}\right)-\epsilon_0 I_m\left(\frac{\omega a}{v}\right)K_m'\left(\frac{\omega a}{v}\right)}\right\},\tag{9}$$

for outside trajectories. Here, e is the charge of the electron, J_m represents the cylindrical Bessel function of the first kind, I_m and K_m are modified Bessel functions, and μ_m are Neumann numbers. The energy loss probability of Eqs. (8) and (9) is in agreement with previous results [4,5,7] obtained by following a classical approach.

At this point we consider the following representation [21]:

$$\int_0^\infty {\rm d}x\,\frac{x}{x^2+c^2}\,J_m(ax)J_m(bx)$$

$$=\begin{cases}I_m(ac)K_m(bc), & \text{if } a\le b;\\ I_m(bc)K_m(ac), & \text{otherwise}\end{cases}\tag{10}$$

we also take advantage of the identity:

$$\sum_{m=0}^{\infty}\mu_m J_m^2(x)=1,\tag{11}$$

we average Eqs. (8) and (9) over impact parameters and, finally, we equate the resulting energy loss probability with that of swift electrons passing through a homogeneous medium of non-local dielectric function $\epsilon(\boldsymbol{q},\omega)$ [22],

$$P_\omega=-\frac{e^2}{\pi^2}\int\frac{{\rm d}\boldsymbol{q}}{q^2}\,{\rm Im}\,[\epsilon^{-1}(\boldsymbol{q},\omega)-1]\delta[\hbar\omega-(E_0-E_f)],\tag{12}$$

to obtain the following result for the momentum-dependent effective inverse longitudinal dielectric function of a system of independent cylinders in an otherwise homogeneous medium:

$$\epsilon_{\rm eff}^{-1}(\boldsymbol{q},\omega)=\epsilon_0^{-1}+f(\epsilon_\omega^{-1}-\epsilon_0^{-1})$$

$$\times\left\{1+\frac{2}{(Qa)^2+(q_z a)^2}\sum_{m=0}^{\infty}\mu_m J_m(Qa)\right.$$

$$\left.\times\frac{\epsilon_\omega I_m'(q_z a)f_m^{(1)}+\epsilon_0 K_m'(q_z a)f_m^{(2)}}{\epsilon_\omega I_m'(q_z a)K_m(q_z a)-\epsilon_0 I_m(q_z a)K_m'(q_z a)}\right\},\tag{13}$$

where

$$f_m^{(1)}=q_z a J_m(Qa)K_{m-1}(q_z a)+Qa J_{m-1}(Qa)K_m(q_z a).\tag{14}$$

$$f_m^{(2)}=q_z a J_m(Qa)I_{m-1}(q_z a)-Qa J_{m-1}(Qa)I_m(q_z a).\tag{15}$$

f represents the relative part of the total volume

occupied by the cylinder, $\boldsymbol{Q}$ is a vector located in a plane perpendicular to the z axis, and $q_z=\omega/v$.

2.2. Broad beam geometries

We now consider a broad beam geometry, and we therefore use, plane waves to describe the electron states:

$$\phi_0(\boldsymbol{r})=\frac{1}{\sqrt{\Omega}}\,e^{i\boldsymbol{q}_0\cdot\boldsymbol{r}} \tag{16}$$

and

$$\phi_f(\boldsymbol{r})=\frac{1}{\sqrt{\Omega}}\,e^{i\boldsymbol{q}_f\cdot\boldsymbol{r}}, \tag{17}$$

where Ω represents the normalization volume.

Then, introduction of Eqs. (16) and (17) into Eq. (6) leads to the following result:

$$P_\omega=-\frac{2}{\Omega}\int\frac{d\boldsymbol{q}}{(2\pi)^3}\int d\boldsymbol{r}\int d\boldsymbol{r}'\,e^{-i\boldsymbol{q}\cdot(\boldsymbol{r}-\boldsymbol{r}')}\times \mathrm{Im}\,W^{\mathrm{ind}}(\boldsymbol{r},\boldsymbol{r}';\omega)\delta[\hbar\omega-(E_0-E_f)], \tag{18}$$

where $\boldsymbol{q}$ represents the momentum transfer:

$$\boldsymbol{q}=\boldsymbol{q}_0-\boldsymbol{q}_f. \tag{19}$$

Thus, equating the energy loss probability of Eq. (18) with that of Eq. (12) gives the following expression for the inverse longitudinal dielectric function:

$$\epsilon_{\mathrm{eff}}^{-1}(\boldsymbol{q},\omega)=(1-f)\epsilon_0^{-1}+f\epsilon_\omega^{-1}+\frac{q^2}{4\pi e^2\Omega}\times\int d\boldsymbol{r}\int d\boldsymbol{r}'\,e^{-i\boldsymbol{q}\cdot(\boldsymbol{r}-\boldsymbol{r}')}W^{\mathrm{s}}(\boldsymbol{r},\boldsymbol{r}';\omega), \tag{20}$$

where $W^{\mathrm{s}}(\boldsymbol{r},\boldsymbol{r}';\omega)$ represents the contribution to the screened interaction coming from the charge induced at the interface. Eq. (20) does not depend on the direction of the external beam.

The contribution $W^{\mathrm{s}}(\boldsymbol{r},\boldsymbol{r}';\omega)$ to the screened interaction is obtained after imposing the boundary conditions at the surface, and we also introduce the following expansion of a plane wave [23]:

$$e^{i\boldsymbol{Q}\cdot\boldsymbol{\rho}}=\sum_{m=0}^{\infty}\mu_m i^m J_m(Q\rho)\cos m\phi, \tag{21}$$

where $\boldsymbol{Q}$ and ρ represent vectors located in a plane perpendicular to the axis of the cylinder, ϕ being the angle between them. Then, introduction of Eq. (21) into Eq. (20) gives Eq. (13) for the effective inverse longitudinal dielectric function.

Eq. (13) was obtained in the previous subsection by assuming that electrons move in a direction parallel to the axis of the cylinder, the component of the momentum transfer in this direction equalling, therefore, ω/v. However, Eq. (13) is now obtained for any direction of the broad beam, q_z being the component of the momentum transfer, $\boldsymbol{q}$, in the direction of the axis of the cylinder, and q_z does not any longer necessarily equal ω/v. Eq. (13) also coincides exactly with the result one obtains by following a mean field theory of the effective response [15].

3. Spectral representation for $\epsilon_{\mathrm{eff}}^{-1}(q,\omega)$

The quantities in Eq. (13) can be simplified and combined to find, after some algebra, the following expression for the effective inverse longitudinal dielectric function of isolated cylinders:

$$\epsilon_{\mathrm{eff}}^{-1}(\boldsymbol{q},\omega)=(1-f)\epsilon_0^{-1}+f\left\{\epsilon_\omega^{-1}+\sum_{m=0}^{\infty}C_m\times\left[(1-n_m^{-1})\epsilon_0^{-1}-\epsilon_\omega^{-1}+\frac{n_m^{-1}}{\epsilon_\omega n_m+\epsilon_0(1-n_m)}\right]\right\}, \tag{22}$$

where C_m and n_m represent surface mode strengths and positions, respectively:

$$C_m=\frac{2q_za}{(Qa)^2+(q_za)^2}\,\mu_m J_m^2(Qa)I_m'(q_za)I_m^{-1}(q_za) \tag{23}$$

and

$$n_m=q_zaI_m'(q_za)K_m(q_za). \tag{24}$$

The first and second terms in the right-hand side of Eq. (22) represent contributions to the bulk modes of the host and the cylinder, respectively, coming from the charge induced in the interior of both media. The third and fourth terms represent

the so-called Begrenzung effect in the host and the cylinder, i.e., the contribution to bulk modes appearing as a consequence of the presence of the surface. The last term gives account of the surface modes of the system.

Now, we follow Ref. [14] to introduce a new variable,

$$u=(1-\epsilon_\omega/\epsilon_0)^{-1}, \tag{25}$$

into Eq. (22), and we find the following spectral representation:

$$\epsilon_{\rm eff}^{-1}(\boldsymbol{q},\omega)=\epsilon_0^{-1}\left\langle 1+f\left\{(u-1)^{-1}+\sum_{m=0}^{\infty} C_m[-(u-1)^{-1}+(u-n_m)^{-1}]\right\}\right\rangle, \tag{26}$$

where surface mode strengths and positions are given by Eqs. (23) and (24), respectively.

Eq. (26) is new. The spectral representation for the effective inverse dielectric function of a composite system was first introduced by Bergman [24] and Milton [25] in the $q=0$ limit, and it was extended by Barrera and Fuchs [14] to finite wavevectors in a system of identical spheres. Eq. (26) represents the spectral representation for the effective inverse longitudinal dielectric function of a system of independent cylinders in an otherwise homogeneous medium.

In particular, if the momentum transfer is parallel to the axis of the cylinder, i.e., $Qa=0$, all surface mode strengths are zero except from C_0:

$$C_0=2(q_za)^{-1}I_1(q_za)I_0^{-1}(q_za), \tag{27}$$

and the corresponding mode position is given by:

$$n_0=q_zaI_1(q_za)K_0(q_za). \tag{28}$$

In the local limit ($q_za\to 0$) $C_0=1$, and, therefore, the Begrenzung term exactly cancels the bulk mode inside the cylinder. On the other hand, in this limit $n_0=0$, so that the bulk mode of the host dominates unless the dielectric function in the interior of the cylinder goes to infinity.

In the case of a momentum transfer that is located in a plane perpendicular to the axis of the cylinder ($q_za=0$), the zero order mode strength is zero, $C_0=0$, and for $m\neq 0$ one finds:

$$C_m=4(Qa)^{-2}mJ_m^2(Qa), \tag{29}$$

the corresponding mode positions all being equal to the planar mode, $n_{m\neq 0}=1/2$. In the local limit ($Qa\to 0$) only the first order mode strength, $C_{m=1}$, contributes to the multipolar sum of Eq. (26); this mode strength has the value 1, and the Begrenzung term exactly cancels the bulk mode inside the cylinder, so that the planar surface mode dominates. For finite values of the momentum transfer both planar and bulk modes contribute.

Finally, if one assumes that the radius of the cylinder is small, i.e., $Qa\ll 1$ and $q_za\ll 1$, then an expansion of Eq. (26) gives, in the local limit:

$$\epsilon_{\rm eff}^{-1}(\boldsymbol{q},\omega)=\epsilon_0^{-1}\left[1+f\frac{q_z^2(u-n_0)^{-1}+Q^2(u-n_1)^{-1}}{q_z^2+Q^2}\right], \tag{30}$$

where $n_0=0$ and $n_1=1/2$. Eq. (30) shows that in the local limit there is no contribution from the bulk mode inside the cylinder.

In the case of a free electron gas of dielectric function $\epsilon_\omega=1-\omega_p^2/\omega^2$, where ω_p is the plasma frequency, it is straightforward from Eq. (22) or Eq. (26) that $n_m=\omega_m^2/\omega_p^2$, where ω_m represents the eigenfrequencies for the cylindrical surface plasmon modes. Accordingly, the surface mode positions n_m, which are independent of the material inside and outside the cylinder, equal the square of the modes represented in Ref. [7] as a function of q_za.

One easily finds from Eq. (24) that the limiting value for $q_za\gg 1$ equals, for all m, the planar mode, $n_m=1/2$. In the long-wavelength limit, i.e., $q_za\ll 1$, the limiting values are $n_m=1/2$ for $m\neq 0$ and $n_m=0$ for $m=0$, as discussed above. For intermediate values of q_za they are all lower than the planar mode. In particular, $0.41<n_m<0.50$ for $m\neq 0$ and all values of q_za, and n_0 is also larger than 0.41 for $q_za>3.0$. Thus, for large values of the parameter q_za ($q_za>3.0$) all surface mode positions are very close to the planar mode.

In Fig. 1 we show C_0 of Eq. (23) as a function of qa, $\boldsymbol{q}$ being the total momentum transfer, for different values of q_za. When the momentum transfer is perpendicular to the axis of the cylinder,

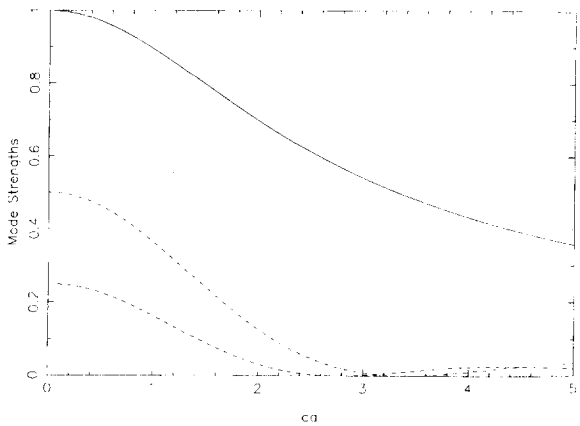

Fig. 1. Zero-order surface mode strength, C_0, of Eq. (23), as a function of qa, for four different values of $q_z a$: $1/2qa$ (dashed line), $\sqrt{2}/2qa$ (dashed-dotted line), $\sqrt{3}/2qa$ (dotted line), and qa (solid line). When $q_z a=0$, $C_0=0$ for all values of qa.

i.e., $q_z a=0$, $C_0=0$ for all values of qa, as noted above. As the value of $q_z a$ increases C_0 also increases for $qa<3.0$, and the limiting value of Eq. (27) is found when $q_z=q$ (solid line); in this case, $C_0=1$ for $qa=0$ and it decreases as $(qa)^2$ for small qa.

The total strength of the surface modes with $m\geq 1$, as obtained from Eq. (23), is plotted in Fig. 2, as a function of qa, also for different values of $q_z a$. When the momentum transfer is perpendicular to the axis of the cylinder ($q_z a=0$), Eq. (23) can be replaced by Eq. (29) and one obtains the result plotted in this figure by a solid line: this curve gives the total strength of the surface modes, it has the value 1 when $qa=0$, and it decreases as $(qa)^2$ for small qa. As the value $q_z a$ increases, the total strength of the surface modes with $m\geq 1$ decreases for small values of qa. In the case of a momentum transfer that is parallel to the axis of the cylinder ($q_z=q$), all strengths with $m\geq 1$ are equal to zero for all values of qa.

In Fig. 3 the total strength of all surface modes is plotted, as a function of qa, for different values of $q_z a$. The bulk mode strength,

$$C_b=1-\sum_{m=0}^{\infty} C_m, \tag{31}$$

has the value 0 when $qa=0$, and is independent of the direction of the momentum transfer for small qa: introduction of Eq. (23) into Eq. (31) gives, up to second order in Qa and $q_z a$ [see also Eq. (30)]:

$$C_b=\tfrac{1}{8}q^2. \tag{32}$$

Fig. 3 also shows that as the value of $q_z a$ increases, the bulk mode decreases and the Begrenzung effect happens, therefore, to become more important.

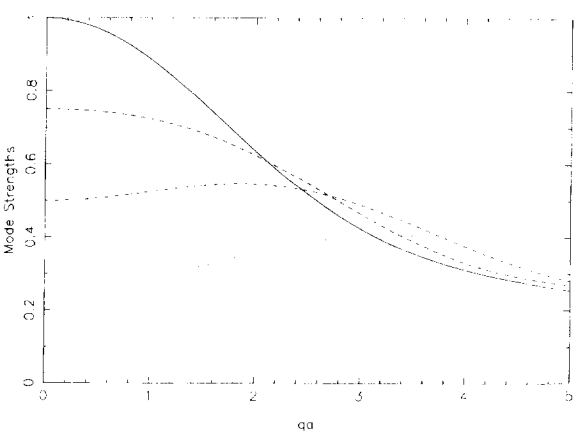

Fig. 2. Total strength of the surface modes with $m\geq 1$, $\sum_{m=1}^{\infty} C_m$, as obtained from Eq. (23), as a function of qa, for four different values of $q_z a$: 0 (solid line), $1/2qa$ (dashed line), $\sqrt{2}/2qa$ (dashed-dotted line), and $\sqrt{3}/2qa$ (dotted line). When $q_z=q$, $C_m=0$ for all $m\neq 0$.

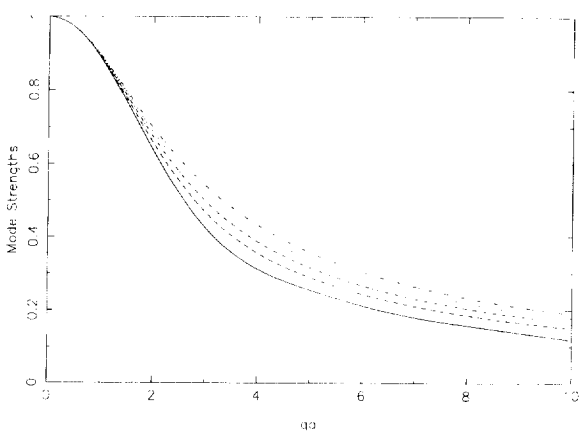

Fig. 3. Total strength of all surface modes, $\sum_{m=0}^{\infty} C_m$, as a function of qa, for five different values of $q_z a$: 0 (solid line), $1/2qa$ (dashed line), $\sqrt{2}/2qa$ (dashed-dotted line), $\sqrt{3}/2qa$ (dotted line), and qa (dashed-dotted-dotted-dotted line).

4. Conclusions

In conclusion, we have used a self-energy formalism to describe the interaction of STEM electrons with cylindrical surfaces. We have derived a general expression for the momentum-dependent effective inverse longitudinal dielectric function of a system of independent cylinders, and we have written this dielectric function in the form of a spectral representation. We have analyzed the surface mode strengths and positions, and we have found that in the local limit the planar mode dominates when the momentum transfer is perpendicular to the axis of the cylinder, while in the case of a momentum transfer that is parallel to the cylinder only the $n_0=0$ mode contributes. This mode, however, represents the dilute limit ($f\to 0$) of the actual mode of a system of parallel cylinders: $n_0=f$. The effect of the interaction between the cylinders can be investigated [26], in the local limit, on the basis of photonic band structure calculations [27]. Work in this direction is now in progress [28].

The role of surface plasmon excitations in the interaction between probes and cylindrical interfaces has been proved [15] to be important in the investigation of the experimental valence-loss spectra from zeolites [29]. Also, the existence of tubular fullerenes opens a new field of applications of this theory.

Acknowledgements

We thank P.M. Echenique and J.B. Pendry for stimulating conversations. The authors also gratefully acknowledge the financial support of the University of the Basque Country, the Basque Unibertsitate eta Ikerketa Saila, the Spanish Comisión Asesora, Científica y Técnica (CAICYT), and the British Council. One of us (J.M.P.) acknowledges the hospitality of the Department of Physics of Imperial College of Science, Medicine and Technology, London, UK, where part of this work was carried out.

References

[1] R.H. Ritchie, Phys. Rev. 106 (1957) 874.
[2] P.M. Echenique and J.B. Pendry, J. Phys. C 8 (1975) 2936.
[3] T.L. Ferrell and P.M. Echenique, Phys. Rev. Lett. 55 (1985) 1526;
T.L. Ferrell, R.J. Warmack, V.E. Anderson and P.M. Echenique, Phys. Rev. B 35 (1987) 7365.
[4] C.A. Walsh, Phil. Mag. 59 (1989) 227.
[5] N. Zabala, A. Rivacoba and P.M. Echenique, Surf. Sci. 209 (1989) 465.
[6] A. Rivacoba, P. Apell and N. Zabala, Nucl. Instrum. Methods B 96 (1995) 465.
[7] M. Schmeits, Phys. Rev. B 39 (1989) 7567.
[8] M. Schmeits and L. Dambly, Phys. Rev. B 44 (1991) 12706.
[9] A. Rivacoba, N. Zabala and P.M. Echenique, Phys. Rev. Lett. 69 (1992) 3362.
[10] J.C. Maxwell-Garnett, Phil. Trans. R. Soc. Lond. 203 (1904) 385; 205 (1906) 237.
[11] F. Fujimoto and K. Komaki, J. Phys. Soc. Jpn. 25 (1968) 1769.
[12] D.R. Penn and P. Apell, J. Phys. C 16 (1983) 5729.
[13] P.M. Echenique, J. Bausells and A. Rivacoba, Phys. Rev. B 35 (1987) 1521.
[14] R.G. Barrera and R. Fuchs, Phys. Rev. B 52 (1995) 3256.
[15] J.M. Pitarke, J.B. Pendry and P.M. Echenique, Phys. Rev. B, to be published.
[16] S. Iijima, Nature 354 (1991) 56.
[17] L.A. Bursill, Pierre A. Stadelmann, J.L. Peng and Steven Prawer, Phys. Rev. B 49 (1994) 2882.
[18] L. Hedin and S. Lundqvist, in Solid State Physics, Eds. F. Seitz, D. Turbull and E.H. Ehrenreich (Academic Press, New York, 1969).
[19] J.J. Quinn and R.A. Ferrell, Phys. Rev. 112 (1958) 812.
[20] R.H. Ritchie, Phys. Rev. 114 (1959) 644.
[21] I.S. Gradshteyn and I.M. Ryzhik, Table of Integrals, Series and Products (Academic Press, New York, 1980).
[22] P.M. Echenique, F. Flores and R.H. Ritchie, in: Solid State Physics, Eds. E.H. Ehrenreich and D. Turbull (Academic Press, New York, 1990).
[23] F. Bowman, Introduction to Bessel Functions (Longmans Green, London, 1938), p. 90.
[24] D. Bergman, Phys. Rep. 43 (1978) 377.
[25] G. Milton, J. Appl. Phys. 52 (1981) 5286.
[26] J.B. Pendry and L. Martín-Moreno, Phys. Rev. B 50 (1994) 5062;
L. Martín Moreno and J.B. Pendry, Nucl. Instrum. Methods. B 96 (1995) 565.
[27] J.B. Pendry and A. MacKinnon, Phys. Rev. Lett. 69 (1992) 2772.
[28] F.J. García Vidal, J.M. Pitarke and J.B. Pendry, to be published.
[29] D.W. McComb and A. Howie, Nucl. Instrum. Methods B 96 (1995) 569.